

*Supporting Information for*

**Europium Coordination Polymers Based on two conjugated  
tetracarboxylates: Syntheses, Structures, Luminescence and  
Magnetic Properties**

Li-Feng Wang,<sup>a,b</sup> Ling-Chen Kang,<sup>a</sup> Wen-Wei Zhang,<sup>\*a</sup> Fang-Ming  
Wang,<sup>a</sup> Xiao-Ming Ren<sup>\*b</sup> and Qing-Jin Meng<sup>a</sup>

<sup>a</sup> *State Key Laboratory of Coordination Chemistry, School of Chemistry and Chemical Engineering, Nanjing University, Nanjing 210093. E-mail: wwzhang@nju.edu.cn*

<sup>b</sup> *Department of Applied Chemistry, College of Science, Nanjing University of Technology, Nanjing 210009. E-mail: xmren@njut.edu.cn*

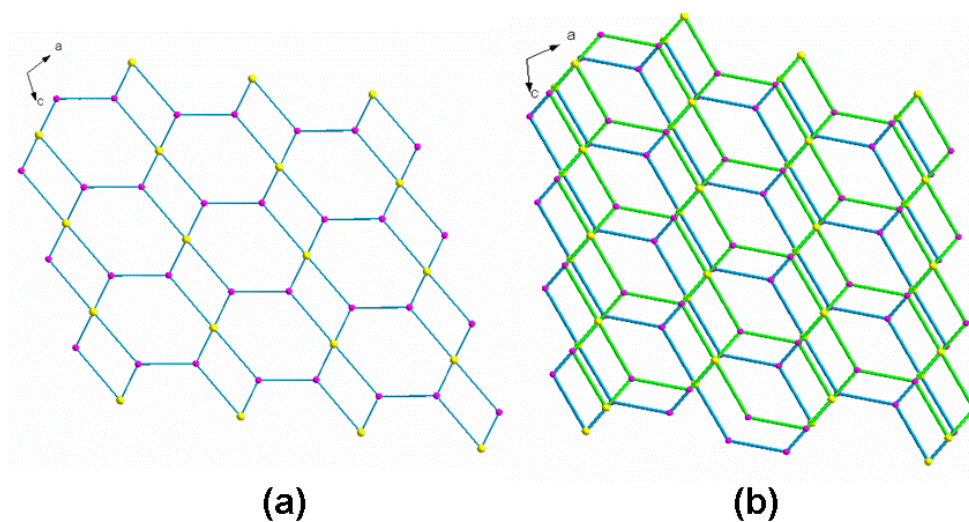


**Fig. S1** Schematic diagram of the extended net with 2D (3,4) topology in complex **1** viewed along the *b* direction: (a) one layer; (b) two adjacent layers (pink: the center of the binuclear unit; orange: the center of the aryl rings).

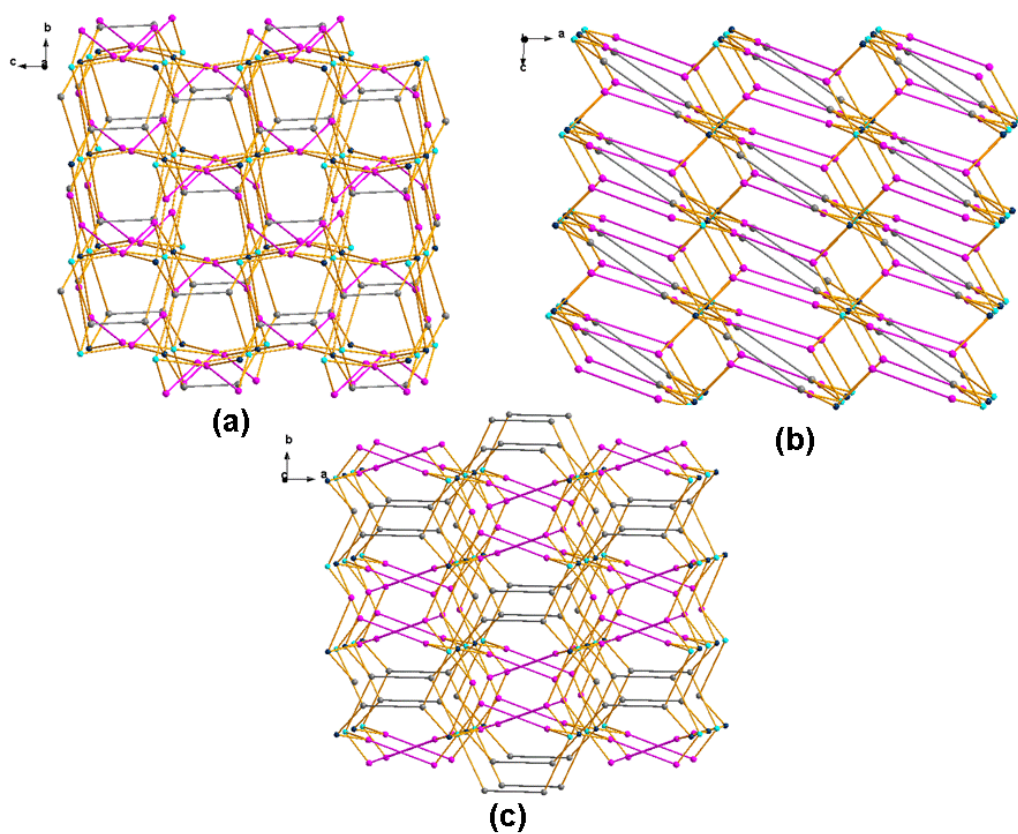
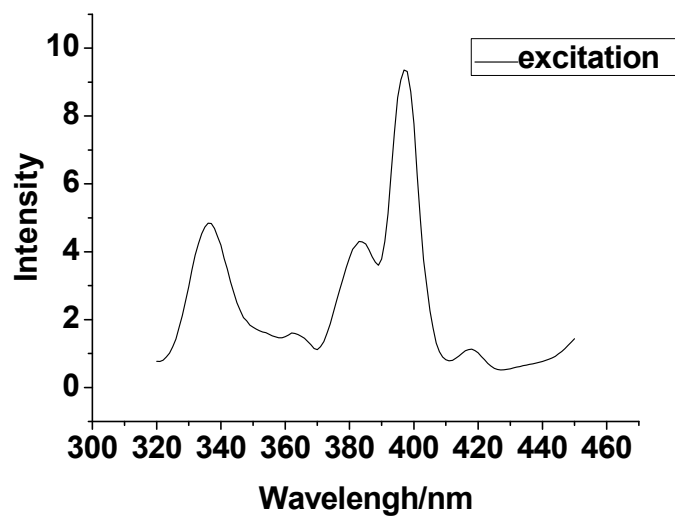
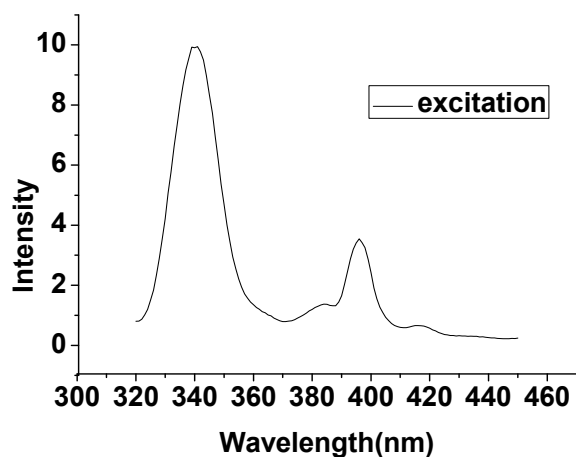


**Fig. S2** Schematic diagram of the stacking net with 3D (3,6) topology in complex **2** along the direction of *a* (a), *b* (b), and *c* (c) (dark teal: the center of  $\text{Eu}_2(\text{CO}_2)_4$  (**A**) subunits; turquoise: the center of  $\text{Eu}_2(\text{CO}_2)_2$  (**B**) subunit; gray: the center of the  $\text{BBTC}^{4-}(\alpha)$  aryl rings; pink: the center of the  $\text{BBTC}^{4-}(\beta)$  aryl rings).



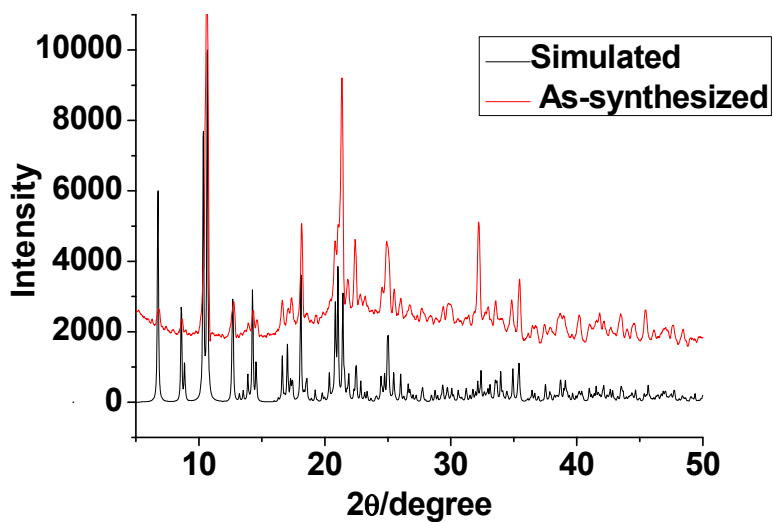
(a)



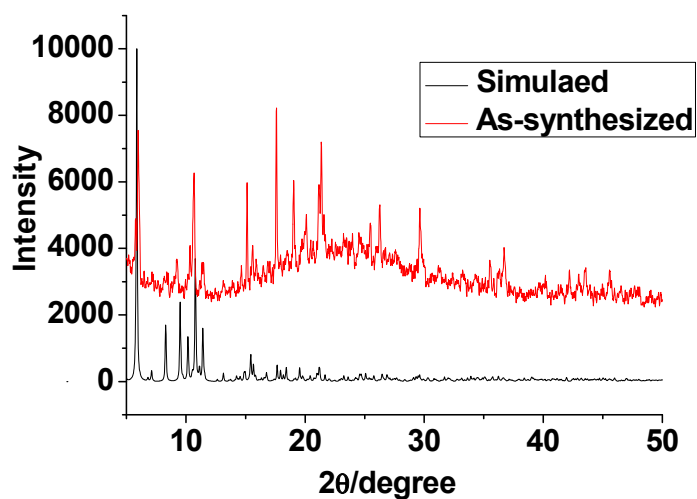
(b)

**Fig. S3** Room-temperature excitation spectra for complex **1** (a) and **2** (b) in solid state.

Complex **1** exhibits excitation bands at 336, 383, 397 and 417 nm, while **2** shows excitation bands at 340 and 397 nm. When excited at 397 nm for **1** and 340 nm for **2**, both of them show characteristic luminescence.



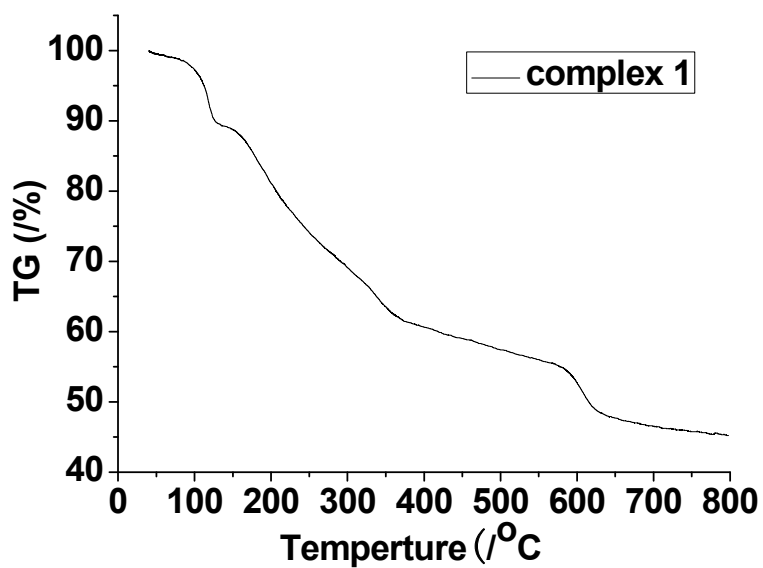
(a)



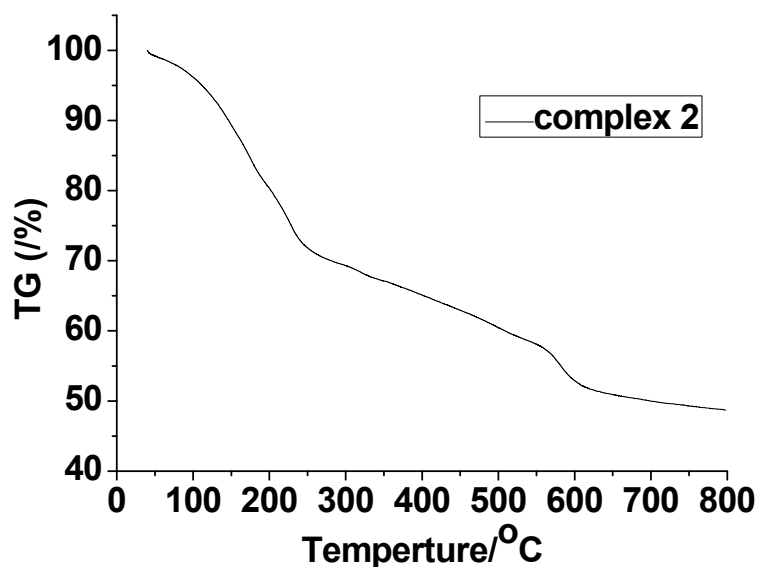
(b)

Fig. S4 PXRD patterns of compound **1** (a) and **2** (b).

The purities of complexes **1** and **2** are confirmed by X-ray power diffraction analyses. The experimental and stimulated powder X-ray diffraction (PXRD) patterns are consistent with each other to indicate the good purity of the samples.



(a)



(b)

Fig. S5 TG curves of compound **1** (a) and **2** (b).

Thermal gravimetric analysis (TGA) was conducted to determine the thermal stabilities of **1** and **2** which is an important aspect for metal-organic frameworks. As shown in Fig. S5, **1** and **2** exhibit several sequential weight loss steps, corresponding to the delibration of guest molecules and coordinated solvents. Above 470 °C for **1** and 520 °C for **2**, the frameworks start to decompose.

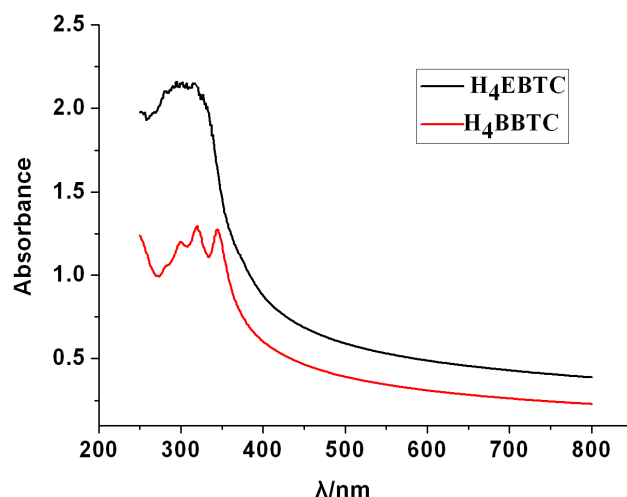


Fig. S6 UV-vis spectra of H<sub>4</sub>EBTC (black) and H<sub>4</sub>BBTC (red).

Table S1. Selected bond distances (Å) and angles(°) for **1**

**Bond distances/ Å**

Eu1–O2	2.336(6)	Eu1–O5	2.345(5)
Eu1–O7	2.477(6)	Eu1–O8	2.442(6)
Eu1–O9	2.530(8)	Eu1–O10	2.519(7)
Eu1–O12	2.534(8)	Eu1–O13	2.507(8)
Eu1–O15	2.351(8)	Eu2–O1	2.303(6)
Eu2–O3	2.465(6)	Eu2–O4	2.436(6)
Eu2–O6	2.338(6)	Eu2–O16	2.360(7)
Eu2–O17	2.434(8)	Eu2–O18	2.455(7)
Eu2–O19	2.381(7)		

**Bond angles/ °**

O2–Eu1–O5	82.6(2)	O2–Eu1–O15	79.2(3)
O5–Eu1–O15	78.3(2)	O2–Eu1–O8	127.4(2)
O5–Eu1–O8	148.4(2)	O15–Eu1–O8	96.0(3)
O2–Eu1–O7	75.6(2)	O5–Eu1–O7	150.7(2)
O15–Eu1–O7	78.7(3)	O8–Eu1–O7	52.4(2)
O2–Eu1–O13	79.9(2)	O5–Eu1–O13	72.1(2)
O15–Eu1–O13	145.6(3)	O8–Eu1–O13	118.4(2)
O7–Eu1–O13	121.6(3)	O2–Eu1–O10	151.0(2)
O5–Eu1–O10	86.0(2)	O15–Eu1–O10	124.3(3)
O8–Eu1–O10	71.5(2)	O7–Eu1–O10	122.2(2)
O13–Eu1–O10	71.2(3)	O2–Eu1–O9	150.7(3)
O5–Eu1–O9	78.4(2)	O15–Eu1–O9	75.2(3)
O8–Eu1–O9	70.1(2)	O7–Eu1–O9	112.7(2)

O13–Eu1–O9	114.4(3)	O10–Eu1–O9	49.2(3)
O2–Eu1–O12	82.8(3)	O5–Eu1–O12	121.7(2)
O15–Eu1–O12	151.0(3)	O8–Eu1–O12	77.2(3)
O7–Eu1–O12	74.9(3)	O13–Eu1–O12	49.8(3)
O10–Eu1–O12	80.7(3)	O9–Eu1–O12	126.3(3)
O1–Eu2–O6	78.7(2)	O1–Eu2–O16	90.1(2)
O6–Eu2–O16	78.6(2)	O1–Eu2–O19	107.8(3)
O6–Eu2–O19	74.7(2)	O16–Eu2–O19	143.9(2)
O1–Eu2–O17	76.8(3)	O6–Eu2–O17	143.5(3)
O16–Eu2–O17	74.9(3)	O19–Eu2–O17	138.8(3)
O1–Eu2–O4	149.8(2)	O6–Eu2–O4	131.46(2)
O16–Eu2–O4	94.4(2)	O19–Eu2–O4	85.6(2)
O17–Eu2–O4	75.7(3)	O1–Eu2–O18	81.3(2)
O6–Eu2–O18	146.7(2)	O19–Eu2–O18	68.7(2)
O17–Eu2–O18	71.8(3)	O4–Eu2–O18	78.7(2)
O1–Eu2–O3	154.7(2)	O6–Eu2–O3	79.30(2)
O16–Eu2–O3	73.5(2)	O19–Eu2–O3	77.9(2)
O17–Eu2–O3	115.7(3)	O4–Eu2–O3	53.1(2)
O18–Eu2–O3	122.8(2)		

**Table S2.** Selected bond distances (Å) and angles(°) for **2**

**Bond distances/ Å**

Eu(1)–O3	2.471(6)	Eu(1)–O4	2.507(6)
Eu(1)–O5	2.396(7)	Eu(1)–O6	2.336(6)
Eu(1)–O9	2.389(6)	Eu(1)–O10	2.322(6)
Eu(1)–O13	2.440(8)	Eu(1)–O14	2.426(8)
Eu(2)–O1	2.306(7)	Eu(2)–O2	2.300(9)
Eu(2)–O7	2.532(6)	Eu(2)–O8	2.390(8)
Eu(2)–O11	2.480(7)	Eu(2)–O12	2.384(7)
Eu(2)–O15	2.355(9)	Eu(2)–O16	2.714(11)

**Bond angles/°**

O3–Eu1–O4	52.2(2)	O5–Eu1–O3	77.2(2)
O5–Eu1–O4	76.8(2)	O5–Eu1–O13	144.1(3)
O5–Eu1–O14	136.0(3)	O6–Eu1–O3	144.0(2)
O6–Eu1–O4	150.6(2)	O6–Eu1–O5	124.8(2)
O6–Eu1–O9	78.2(2)	O6–Eu1–O13	77.4(3)
O6–Eu1–O14	78.9(3)	O9–Eu1–O3	137.6(2)
O9–Eu1–O4	90.0(2)	O9–Eu1–O5	75.8(3)
O9–Eu1–O13	140.0(3)	O9–Eu1–O14	74.1(3)
O10–Eu1–O3	82.0(2)	O10–Eu1–O4	131.5(2)



---

O10–Eu1–O5	78.5(2)	O10–Eu1–O6	76.3(6)
O10–Eu1–O9	123.0(2)	O10–Eu1–O13	80.8(3)
O10–Eu1–O14	145.4(3)	O13–Eu1–O3	71.1(3)
O13–Eu1–O4	96.0(3)	O14–Eu1–O3	105.5(3)
O14–Eu1–O4	71.9(3)	O14–Eu1–O13	70.4(3)
O1–Eu2–O7	77.3(2)	O1–Eu2–O8	82.4(4)
O1–Eu2–O12	149.8(3)	O1–Eu2–O15	79.3(3)
O1–Eu2–O16	90.8(3)	O2–Eu2–O1	93.6(3)
O2–Eu2–O7	128.9(3)	O2–Eu2–O8	77.2(3)
O2–Eu2–O11	77.4(3)	O2–Eu2–O12	105.1(3)
O2–Eu2–O15	79.8(4)	O2–Eu2–O16	158.4(3)
O7–Eu2–O16	72.7(3)	O8–Eu2–O7	51.9(2)
O8–Eu2–O11	113.1(3)	O8–Eu2–O16	124.4(3)
O11–Eu2–O7	122.9(3)	O11–Eu2–O16	91.2(3)
O12–Eu2–O7	72.5(2)	O12–Eu2–O8	79.0(3)
O12–Eu2–O11	50.6(3)	O12–Eu2–O16	80.5(3)
O15–Eu2–O7	143.7(3)	O15–Eu2–O8	149.5(4)
O15–Eu2–O11	80.6(3)	O15–Eu2–O12	126.7(3)
O15–Eu2–O16	80.3(4)		

---